Charm Dalitz Analyses

Gianluca Cavoto

Università di Roma La Sapienza, INFN and Dipartimento di Fisica, I-00185 Roma, Italy

A review of recent experimental results of Dalitz analyses of charmed meson decays into three-body final states is presented. These analyses can help in understanding the strong interaction dynamics leading to the observed light mesons spectrum (low mass scalar σ, $f_0(980)$, $a_0(980)$). A model for the decay amplitude into such states is very important for the extraction of the angle γ of the CKM unitarity triangle. Implications for such measurement are discussed.

1. Introduction

A D meson is as a unique "laboratory" to study light quark spectroscopy. It has a well defined spin-parity $J^P = 0^-$, constraining the angular momentum of the decay products in multibody final states which can be analyzed with the Dalitz plot technique [1].

Investigations of the low mass scalar mesons can be pursued in three-body decays of pseudoscalar D mesons giving their large coupling to such states. The nature of such low mass scalar states is still under discussion [2], since scalar mesons are difficult to resolve experimentally because of their large decay width. There are claims for the existence of broad states close to threshold such as $\kappa(800)$ and $\sigma(500)$ [3]. On the theory side the scalar meson candidates are too numerous to fit in a single $J^{PC} = 0^{++}$ $q\bar{q}$ nonet and therefore alternative interpretations are proposed. For instance, $a_0(980)$ or $f_0(980)$ may be 4-quark states due to their proximity to the $\bar{K}K$ threshold [4].

These hypotheses can be tested through an accurate measurement of branching fractions and couplings to different final states. In addition, comparison between the production of these states in decays of differently flavored charmed mesons $D^0(c\bar{u})$, $D^+(c\bar{d})$ and $D_s^+(c\bar{s})$ [5] can yield new information on their possible quark composition. Another benefit of studying charm decays is that, in some cases, partial wave analyses are able to isolate the scalar contribution almost background free.

Results of D^0 Dalitz analyses can be an input for extracting the CP-violating phase $\gamma = \arg(-V_{ud}V_{ub}^*/V_{cd}V_{cb}^*)$ of the quark mixing matrix by exploiting interference structure in the Dalitz plot from the decay $B^\pm \to D^0 K^\pm$ [6]. Modeling of the $K\pi$ and $\pi\pi$ S-wave in D decays is therefore an important element in such measurement, since the systematic uncertainty on γ due to the Dalitz model is dominated by such components [7]. Model independent approaches using special Dalitz charm analyses are discussed and a projected systematic error on γ in future experiments evaluated.

2. Dalitz analysis formalism

The amplitudes describing D meson weak-decays into three-body final states are dominated by intermediate resonances that lead to highly non-uniform intensity distributions in the available phase space.

Neglecting CP violation in D meson decays, we define the D ($\bar{D}$) decay amplitude $\mathcal{A}$ ($\bar{\mathcal{A}}$) in a $D \to ABC$ Dalitz plot, as:

$$\mathcal{A}[D \to ABC] \equiv f_{D^0}(m_{BC}^2, m_{AC}^2), \qquad (1)$$

$$\bar{\mathcal{A}}[\bar{D} \to BAC] \equiv f_{D^0}(m_{AC}^2, m_{BC}^2). \qquad (2)$$

The complex quantum mechanical amplitude f is a coherent sum of all relevant quasi-two-body $D \to (r \to AB)C$ resonances ("isobar model" [8]), $f = \sum_r a_r e^{i\phi_r} A_r(s)$. Here $s = m_{AB}^2$, and A_r is the resonance amplitude. The coefficients a_r and ϕ_r are usually obtained from a likelihood fit. The probability density function for the signal events is $|f|^2$. Submodes branching fractions ("fit fractions") are defined as

$$f_r = \frac{|a_r|^2 \int |A_r|^2 dm_{AC}^2 dm_{BC}^2}{\sum_{j,r} c_j c_r^* \int A_j A_r^* dm_{AC}^2 dm_{BC}^2}.$$

The fractions f_r do not necessarily add up to 1 because of interference effects among the amplitudes.

For well established resonances of the spin-1 (P-wave) and spin-2 states, the Breit-Wigner amplitude is used

$$A_{BW}(s) = \mathcal{M}_L(s,p) \frac{1}{M_0^2 - s - iM_0\Gamma(s)}, \quad (3)$$

$$\Gamma(s) = \Gamma_0 \left(\frac{M_0}{\sqrt{s}}\right) \left(\frac{p}{p_0}\right)^{2L+1} \left[\frac{\mathcal{F}_L(p)}{\mathcal{F}_L(p_0)}\right]^2, \quad (4)$$

where M_0 (Γ_0) is the resonance mass (width) [9], L is the angular momentum quantum number, p is the momentum of either daughter in the resonance rest frame, and p_0 is the value of p when s $= M_0^2$. The function $\mathcal{F}_L$ is the Blatt-Weisskopf barrier factor [10]: $\mathcal{F}_0 = 1$, $\mathcal{F}_1 = 1/\sqrt{1 + Rp^2}$, and $\mathcal{F}_2 = 1/\sqrt{9 + 3Rp^2 + Rp^4}$, where we take the meson radial parameter R is usually set to 1.5 GeV^{-1} [11]. The spin part of the amplitude, $\mathcal{M}_L$, is defined

as: $\mathcal{M}_0 = M_D^2$, $\mathcal{M}_1 = -2\ \vec{p}_A.\vec{p}_C$, and $\mathcal{M}_2 = \frac{4}{3}$ [$3(\vec{p}_A.\vec{p}_C)^2 - |\vec{p}_A|^2.|\vec{p}_C|^2]\ M_D^{-2}$, where M_D is the nominal D mass, and $\vec{p}_i$ is the 3-momentum of particle i in the resonance rest frame.

The $A_r(s)$ parameterization of the scalar $f_0(980)$ resonance, whose mass, m_{f_0}, is close to the $K\overline{K}$ production threshold, uses the Flatté [12] formula

$$A_{f_0(980)}(m) =$$
$$\frac{1}{m_{f_0}^2 - s^2 - i[g_{f_0\pi\pi}^2\rho_{\pi\pi}(s) + g_{f_0K\overline{K}}^2\rho_{K\overline{K}}(s)]}, \quad (5)$$

where $g_{f_0\pi\pi}$ and $g_{f_0K\overline{K}}$ are the $f_0(980)$ coupling constants of the resonance to the $\pi\pi$ and $K\overline{K}$ final states, and $\rho_{ab}(s) = 2p_a/\sqrt{(s)}$ is a phase space factor, calculated for the decay products momentum, p_a, in the resonance rest frame. A similar formula is used for the $a_0(980)$ scalar resonance.

Different models for the low mass $\pi\pi$ S wave, (called σ or $f_0(600)$) are used. In [3] a simple spin-0 Breit-Wigner is tried. Alternatively a complex pole amplitude proposed in Ref. [13] can be used

$$A_\sigma(m) = \frac{1}{m_\sigma^2 - m^2}, \quad (6)$$

where $m_\sigma = (0.47 - i0.22)$ GeV is a pole position in the complex s plane estimated from the results of several experiments.

More comprehensive parameterizations of the low mass $\pi\pi$ S wave has been proposed and tested [14] [15]. A K-matrix approach [16, 17], which gives a description of S wave $\pi\pi$ resonances treating the σ and $f_0(980)$ contributions in a unified way has been used giving comparable results to the isobar technique [18].

3. $\pi\pi$ S-wave.

3.1. CLEO-c $D^- \to \pi^+\pi^-\pi^-$

A study of charged D decay to three charged pions has been carried out with the CLEO detector [19]. This mode has been studied previously by E687 [20], E691 [21], E791 [3], and FOCUS [18].

E791 uses the isobar technique, where each resonant contribution to the Dalitz plot is modeled as a Breit-Wigner amplitude with a complex phase. This works well for narrow, well separated resonances, but when the resonances are wide and start to overlap, solutions become ambiguous, and unitarity is violated. In contrast, FOCUS uses the K-matrix approach. The two techniques give a good description of the observed Dalitz plots and agree about the overall contributions of the resonances. Both experiments see that about half of the fit fraction for this decay is explained by a low $\pi^+\pi^-$ mass S wave.

The CLEO analysis utilizes 281 pb^{-1} of data collected on the $\psi(3770)$ resonance at $\sqrt{s} \simeq 3773$ MeV at the Cornell Electron Storage Ring, corresponding to a production of about 0.78×10^6 D^+D^- pairs. D^+ mesons are produced close to the threshold, and are thus almost at rest. Events from the decay $D^+ \to K_S^0\pi^+$, which has a large rate and contributes to the same final state, are isolated with the $\pi^+\pi^-$ invariant mass even without clearly detached vertexes as in the fixed target experiments.

An isobar model is used to parametrize the signal decay where the description of the σ from Ref. [13] and the Flatté parameterization for the threshold effects on the $f_0(980)$ [12] are included. Alternative models are also tried and give comparably good fit results [14] [15].

The $D^+ \to \pi^-\pi^+\pi^+$ decay tracks are selected with requirements on their impact parameters with respect to the beam spot. This removes $\sim 60\%$ of events with $K_S^0 \to \pi^+\pi^-$ decays. The remaining events from $D^+ \to K_S^0\pi^+$ represent about one third of those selected for the Dalitz plot. Selection of events from the $D^+ \to \pi^-\pi^+\pi^+$ decay is done with two signal variables: $\Delta E = E_D - E_{\text{beam}}$ and $m_{\text{BC}} = \sqrt{E_{\text{beam}}^2 - p_D^2}$, where E_{beam} is a beam energy, and E_D and p_D are the energy and momentum of the reconstructed D meson candidate, respectively. This gives 6991 events in the signal box, 2159±18 of these estimated to be background.

The presence of two π^+ mesons impose a Bose-symmetry of the $\pi^-\pi^+\pi^+$ final state. The Bose-symmetry when interchanging the two same sign charged pions is explicitly accounted for in the amplitude parameterization. Dalitz plot is analyzed by choosing $x \equiv m^2(\pi^+\pi^-)_{\text{Low}}$ and $y \equiv m^2(\pi^+\pi^-)_{\text{High}}$ as the independent (x,y) variables. The third variable $z \equiv m^2(\pi^+\pi^+)$ is dependent on x and y through the energy-momentum balance equation.

In the Dalitz plot analysis events in the band $0.2 < m^2(\pi^+\pi^-)_{\text{Low}} < 0.3$ $(\text{GeV}/c^2)^2$ are excluded which is approximately ten times our $K_S^0 \to \pi^+\pi^-$ mass resolution. This leaves for the Dalitz plot analysis 4086 events ~ 2600 of which are signal events.

CLEOc was able to reproduce the fit results E791 [3]. The amplitude normalization and sign conventions are different from E791, in particular the inclusion of a $\sigma\pi$ contribution gives a fit probability of $\simeq 20\%$. Possible contributions form all known $\pi^+\pi^-$ resonances listed in Ref. [22] were tried, including high mass resonances giving asymptotic "tails" at the edge of the kinematically allowed region.

For the $f_0(980)$ the Flatté formula, Eq. 5, is used with parameters taken from the recent BES II measurement [23]. For the σ a complex pole amplitude, Eq. 6, was eventually tried rather than the spin-0 Breit-Wigner.

Table I shows the list of surviving contributions with their fitted amplitudes and phases, and calcu-

Table I Results of the isobar model analysis of the $D^+ \rightarrow \pi^-\pi^+\pi^+$ Dalitz plot. For each contribution the relative amplitude, phase, and fit fraction is given. The errors are statistical and systematic, respectively.

Mode	Amplitude (a.u.)	Phase (°)	Fit fraction (%)
$\rho(770)\pi^+$	1(fixed)	0(fixed)	$20.0\pm2.3\pm0.9$
$f_0(980)\pi^+$	$1.4\pm0.2\pm0.2$	$12\pm10\pm5$	$4.1\pm0.9\pm0.3$
$f_2(1270)\pi^+$	$2.1\pm0.2\pm0.1$	$-123\pm6\pm3$	$18.2\pm2.6\pm0.7$
$f_0(1370)\pi^+$	$1.3\pm0.4\pm0.2$	$-21\pm15\pm14$	$2.6\pm1.8\pm0.6$
$f_0(1500)\pi^+$	$1.1\pm0.3\pm0.2$	$-44\pm13\pm16$	$3.4\pm1.0\pm0.8$
σ pole	$3.7\pm0.3\pm0.2$	$-3\pm4\pm2$	$41.8\pm1.4\pm2.5$

lated fit fractions after a procedure of addition and removal of resonances to improve the consistency between the model and data. The sum of all fit fractions is 90.1%, and the fit probability is $\simeq$28% for 90 degrees of freedom. The two projections of the Dalitz plot and selected fit components are shown in Fig. 1.

For contributions that are not significant upper limits at the 95% confidence level are set.

The systematic uncertainties, shown in Table I, are estimated from numerous fit variations, by adding or removing degrees of freedom, changing the event selection, and varying the efficiency and background parameterizations.

For the poorly established resonances as the σ pole, their parameters are allowed to float and the variations of the other fit parameters contribute to the systematic errors. The fitted values for the σ pole are $Re(m_\sigma)$ (MeV/c^2) = 466$\pm$18 and $Im(m_\sigma)$ (MeV/c^2) = -223 ± 28.
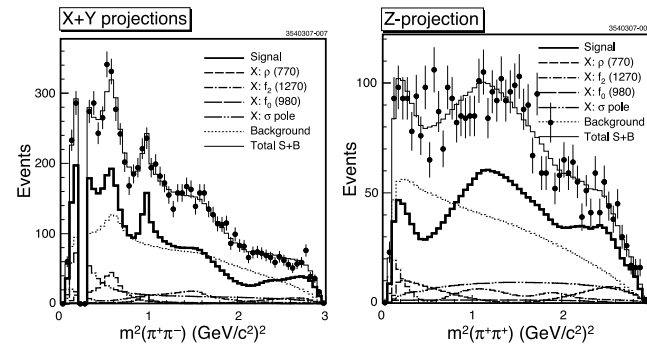

Figure 1: Projection of the Dalitz plot onto the $m^2(\pi^+\pi^-)$ axis (two combinations per D^+ candidate) for CLEO-c data (points) and isobar model fit (histograms) showing the various components (left).Projection of the Dalitz plot onto the $m^2(\pi^+\pi^+)$ axis (right).

3.2. BaBar $D_s \rightarrow K^+K^-\pi^+$

BaBar analyzed 240 fb^{-1} taken at the center of mass energies near the $\Upsilon(4S)$ resonance. Events are

selected in a sample of events having at least three reconstructed charged tracks with two well identified kaons and one pion. The three tracks are fit to a common vertex with the constraint they come from the beamspot. The decay chain $D_s^*(2112)^+ \rightarrow D_s^+\gamma$ helps in discriminating signal from combinatorial background. Additional requirements based on kinematic and geometric information are combined to further suppress the background. The final sample contains 100850 events with a purity of 95%. An unbinned maximum likelihood fit of the Dalitz plot (Fig.2) is performed to extract the relative amplitudes and phases of the intermediate resonances as shown in Tab. II. The decay is dominated by the $\phi(1020)\pi^+$ and $f_0(980)\pi^+$. The $f_0(980)$ is parametrized with a coupled channel Breit-Wigner [23] and its contribution is large but it is subject to a large systematic error due to the poor knowledge of its parameters and possible $a_0(980)$ contributions that are difficult to disentangle in the $K\bar{K}$ projection. Analysis of the angular moment distribution confirms such picture with a big S-wave–P-wave interference in the $K\bar{K}$ channel in the region of the $\phi(1020)$. On the other hand very small activity is present in the $K^*(892)$ region suggesting a small $K\pi$ S-wave, and therefore no evidence of a $\kappa(800)$.
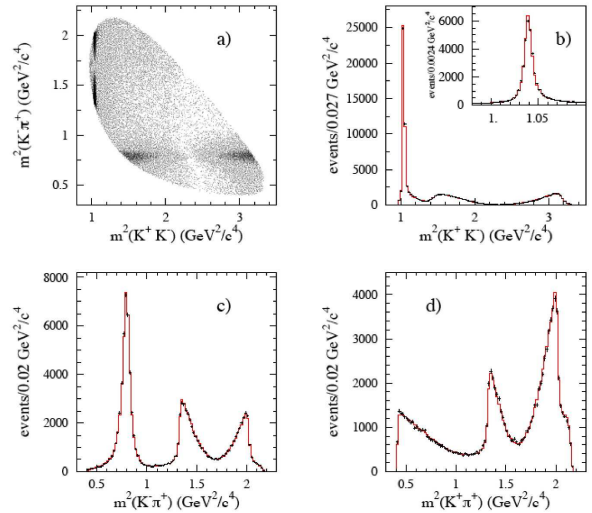

Figure 2: Dalitz plot of $D_s \rightarrow \pi^+K^+K^-$

3.3. BaBar $D^0 \rightarrow \bar{K}^0K^-K^+$

The data sample used in the BaBar $D^0 \rightarrow \bar{K}^0K^-K^+$ analysis consists of 91.5 fb^{-1} recorded with the BaBar detector at the SLAC PEP-II storage rings [24] . The PEP-II facility operates nominally at the

Table II Results of the isobar model analysis of the $D_s \to K^+K^-\pi^+$ Dalitz plot. For each contribution the relative amplitude, phase, and fit fraction is given. The errors are statistical and systematic, respectively.

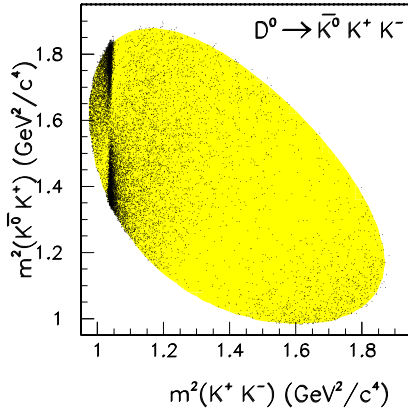| Mode	Amplitude (a.u.)	Phase (°)	Fit fraction (%)
$K^*(892)K^+$	1(fixed)	0(fixed)	$48.7 \pm 0.2 \pm 1.6$
$\phi(1020)\pi^+$	$1.081 \pm 0.006 \pm 0.049$	$2.56 \pm 0.02 \pm 0.38$	$37.9 \pm 0.2 \pm 1.8$
$f_0(980)\pi^+$	$4.6 \pm 0.1 \pm 1.6$	$-1.04 \pm 0.04 \pm 0.48$	$35 \pm 1 \pm 14$
$K_0^*(1430)^0 K^+$	$1.07 \pm 0.06 \pm 0.73$	$-1.37 \pm 0.05 \pm 0.81$	$2.0 \pm 0.2 \pm 3.3$
$f_0(1710)\pi^+$	$0.83 \pm 0.02 \pm 0.18$	$-2.11 \pm 0.05 \pm 0.42$	$2.0 \pm 0.1 \pm 1.0$
$f_0(1370)\pi^+$	$1.74 \pm 0.09 \pm 1.05$	$-2.6 \pm 0.1 \pm 1.1$	$6.3 \pm 0.6 \pm 4.8$
$K_2^*(1430)^0 K^+$	$0.43 \pm 0.05 \pm 0.34$	$-2.5 \pm 0.1 \pm 0.3$	$0.17 \pm 0.05 \pm 0.30$
$f_2(1270)\pi^+$	$0.40 \pm 0.04 \pm 0.35$	$0.3 \pm 0.2 \pm 0.5$	$0.18 \pm 0.03 \pm 0.40$
Sum	$132 \pm 1 \pm 16$		

Figure 3: Dalitz plot of $D^0 \to \overline{K}^0 K^+ K^-$.

$\Upsilon(4S)$ resonance, providing collisions of 9.0 GeV electrons on 3.1 GeV positrons. The data set includes 82 fb^{-1} collected in this configuration (on-resonance) and 9.6 fb^{-1} collected at a c.m. energy 40 MeV below the $\Upsilon(4S)$ resonance (off-resonance).

Selecting events within $\pm 2\sigma$ of the fitted D^0 mass value, a signal fraction of 97.3% is obtained for the 12540 events selected. The Dalitz plot for these $D^0 \to \overline{K}^0 K^+ K^-$ candidates is shown in Fig. 3. In the K^+K^- threshold region, a strong $\phi(1020)$ signal is observed, together with a rather broad structure. A large asymmetry with respect to the $\overline{K}^0 K^+$ axis can also be seen in the vicinity of the $\phi(1020)$ signal, which is most probably the result of interference between S and P-wave amplitude contributions to the K^+K^- system. The $f_0(980)$ and $a_0(980)$ S-wave resonances are, in fact, just below the K^+K^- threshold, and might be expected to contribute in the vicinity of $\phi(1020)$. An accumulation of events due to a charged

$a_0(980)^+$ can be observed on the lower right edge of the Dalitz plot. This contribution, however, does not overlap with the $\phi(1020)$ region and this allows the K^+K^- scalar and vector components to be separated using a partial wave analysis in the low mass K^+K^- region.

The helicity angle, θ_K, is then defined as the angle between the K^+ for D^0 (or K^- for $\overline{D}^0$) in the K^+K^- rest frame and the K^+K^- direction in the D^0 (or $\overline{K}^0$) rest frame. The K^+K^- mass distribution has been modified by weighting each D^0 candidate by the spherical harmonic $Y_L^0(\cos\theta_K)$ (L=0-4) divided by its (Dalitz-plot-dependent) fitted efficiency. It is found that all the $\langle Y_L^0 \rangle$ moments are small or consistent with zero, except for $\langle Y_0^0 \rangle$, $\langle Y_1^0 \rangle$ and $\langle Y_2^0 \rangle$.

In order to interpret these distributions a simple partial wave analysis has been performed, involving only S- and P-wave amplitudes. This results in the following set of equations [25]:

$$\sqrt{4\pi}\left\langle Y_0^0 \right\rangle = S^2 + P^2$$

$$\sqrt{4\pi}\left\langle Y_1^0 \right\rangle = 2\mid S \mid\mid P \mid \cos\phi_{SP} \qquad (3)$$

$$\sqrt{4\pi}\left\langle Y_2^0 \right\rangle = \frac{2}{\sqrt{5}}P^2,$$

where S and P are proportional to the size of the S- and P-wave contributions and ϕ_{SP} is their relative phase. Under these assumptions, the $\langle Y_2^0 \rangle$ moment is proportional to P^2 so that it is natural that the $\phi(1020)$ appears free of background, as is observed. This distribution has been fit using the following relativistic P-wave Breit-Wigner, yielding the following parameters:

$$m_\phi = 1019.63 \pm 0.07, \Gamma_\phi = 4.28 \pm 0.13 \text{ MeV}/c^2$$

in agreement with PDG values (statistical errors only).

The above system of equations can be solved directly for S^2, P^2 and $\cos\phi_{SP}$ and corrected for phase space distribution. The phase space corrected spectra are shown in Fig. 4.

The distributions have been fitted using a model with $\phi(1020)$ for the P-wave , a scalar contribution in the K^+K^- mass projection entirely due to the $a_0(980)^0$, $\overline{K}^0 K^+$ mass distribution is entirely due to $a_0(980)^+$ and the $\cos\phi_{SP}$ described with BW models.

The $a_0(980)$ scalar resonance has a mass very close to the $\bar{K}K$ threshold and decays mostly to $\eta\pi$. It has been described by a coupled channel Breit Wigner of the form:

$$BW_{ch}(a_0)(m) = \frac{g_{\bar{K}K}}{m_0^2 - m^2 - i(\rho_{\eta\pi} g_{\eta\pi}^2 + \rho_{\bar{K}K} g_{\bar{K}K}^2)} \quad (5)$$

where $\rho(m) = 2q/m$ while $g_{\eta\pi}$ and $g_{\bar{K}K}$ describe the $a_0(980)$ couplings to the $\eta\pi$ and $\bar{K}K$ systems respectively.

The best measurements of the $a_0(980)$ parameters come from the Crystal Barrel experiment [26], in $\bar{p}p$ annihilations, with a value of $g_{\bar{K}K} = 329 \pm 27$ $(\text{MeV})^{1/2}$. m_0 and $g_{\eta\pi}$ have been fixed to the Crystal Barrel measurements, but $g_{\bar{K}K}$, on the other hand, has been fit (stat only) $g_{\bar{K}K} = 464 \pm 29$ $(\text{MeV})^{1/2}$.

The determination of $g_{\bar{K}K}$ has been redone in a complete Dalitz plot analysis with an evaluation of the systematic error. The fit produces a reasonable representation of the data for all of the projections. The χ^2 computed on the Dalitz plot gives a value of $\chi^2/NDF=983/774$. The sum of the fractions is $130.7 \pm 2.2 \pm 8.4\%$. The regions of higher χ^2 are distributed rather uniformly on the Dalitz plot. Attempts to improve the fit quality by including other scalar amplitudes caused the fit to diverge, producing a sum of fractions well above 200% along with small improvements of the fit quality.

The final fit results showing fractions, amplitudes and phases are summarised in Table III. For $\overline{K}^0 f_0(980)$ and $K^+ a_0(980)^-$ (DCS), being consistent with zero, only the fractions have been tabulated. For the Dalitz plot analysis the $f_0(980)$ contribution is found to be consistent with zero,

A test has been performed by leaving $g_{\bar{K}K}$ as a free parameter in the Dalitz plot analysis, the resulting central value of $g_{\bar{K}K}$ being

$$g_{\bar{K}K} = 473 \pm 29 \text{ (stat.)} \pm 40 \text{ (syst.)} (\text{MeV})^{1/2}.$$

This value differs significantly from the Crystal Barrel measurement. An improvement of this measurement can be foreseen by adding data from the $a_0(980) \to \eta\pi$ decay mode such as $D^0 \to K_s^0 \eta\pi^0$.

It must be noticed that reliable estimate of the expected contribution of the $f_0(980)$ in $D^0 \to \overline{K}^0 K^+ K^-$ decay is not possible until more accurate measurements of the $f_0(980)$ parameters and couplings become available. This can be performed, for example,

by using high statistics samples of $D_s^+ \to \bar{K}K\pi^+$ and $D_s^+ \to \pi^+\pi^+\pi^-$ decays.
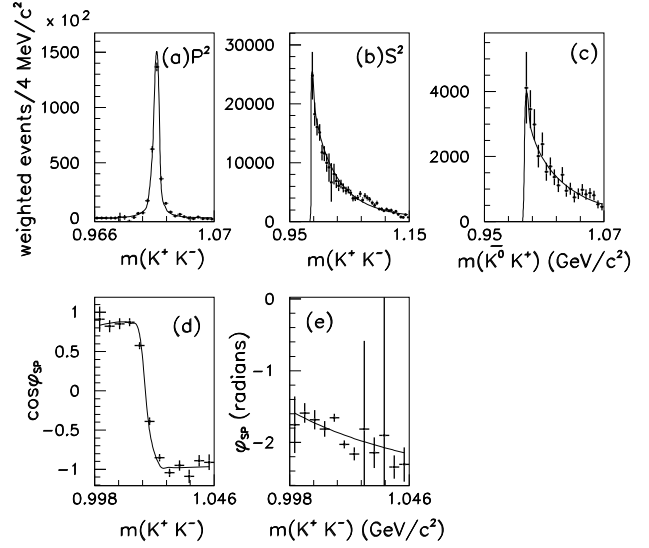

Figure 4: Results from the K^+K^- Partial Wave Analysis corrected for phase space. (a) P-wave strength, (b) S-wave strength. (c) $m(\overline{K}^0 K^+)$ distribution, (d) $\cos\phi_{SP}$ in the $\phi(1020)$ region. (e) ϕ_{SP} in the threshold region after having subtracted the fitted $\phi(1020)$ phase motion shown in (d). The lines correspond to the fit described in the text.

4. $K\pi$ S-wave

The $K^\pm\pi^0$ systems from the decay $D^0 \to K^-K^+\pi^0$ can provide information on the $K\pi$ S-wave (spin-0) amplitude in the mass range 0.6–1.4 GeV/c^2, and hence on the possible existence of the $\kappa(800)$, reported to date only in the neutral state $(\kappa^0 \to K^-\pi^+)$ [3]. If the κ has isospin 1/2, it should be observable also in the charged states.

4.1. BaBar $D^0 \to K^+K^-\pi^0$

BaBar analyzed 385 fb^{-1} of e^+e^- collision data and reconstructed the decays $D^{*+} \to D^0\pi^+$ with $D^0 \to K^-K^+\pi^0$ [27]. Requirements on the center-of-mass momentum of the D^0 candidate and on $|m_{D^{*+}} - m_{D^0}|$ yields in the signal region, $1855 < m_{D^0} < 1875$ MeV/c^2 11278 ± 110 signal events with a purity of about 98.1%.

For D^0 decays to $K^\pm\pi^0$ S-wave states, three amplitude models have been considered. One model uses

Table III Results from the Dalitz plot analysis of $D^0 \to \overline{K}^0 K^+ K^-$. The fits have been performed using the value of $g_{\bar{K}K} = 464$ (MeV)$^{1/2}$ resulting from the partial wave analysis.

Final state	Amplitude	Phase (radians)	Fraction (%)
$\overline{K}^0 a_0(980)^0$	1.	0.	$66.4 \pm 1.6 \pm 7.0$
$\overline{K}^0 \phi(1020)$	$0.437 \pm 0.006 \pm 0.060$	$1.91 \pm 0.02 \pm 0.10$	$45.9 \pm 0.7 \pm 0.7$
$K^- a_0(980)^+$	$0.460 \pm 0.017 \pm 0.056$	$3.59 \pm 0.05 \pm 0.20$	$13.4 \pm 1.1 \pm 3.7$
$\overline{K}^0 f_0(1400)$	$0.435 \pm 0.033 \pm 0.162$	$-2.63 \pm 0.10 \pm 0.71$	$3.8 \pm 0.7 \pm 2.3$
$\overline{K}^0 f_0(980)$			$0.4 \pm 0.2 \pm 0.8$
$K^+ a_0(980)^-$			$0.8 \pm 0.3 \pm 0.8$
Sum			$130.7 \pm 2.2 \pm 8.4$

Table IV The results obtained from the $D^0 \to K^- K^+ \pi^0$ Dalitz plot fit. We define amplitude coefficients, a_r and ϕ_r, relative to those of the $K^*(892)^+$. The errors are statistical and systematic, respectively. We show the $a_0(980)$ contribution, when it is included in place of the $f_0(980)$, in square brackets. We denote the $K\pi$ S-wave states here by $K^\pm \pi^0(S)$.

State	Amplitude, a_r	Phase, ϕ_r (°)	Fraction, f_r (%)
$K^*(892)^+$	1.0 (fixed)	0.0 (fixed)	$45.2 \pm 0.8 \pm 0.6$
$K^*(1410)^+$	$2.29 \pm 0.37 \pm 0.20$	$86.7 \pm 12.0 \pm 9.6$	$3.7 \pm 1.1 \pm 1.1$
$K^+ \pi^0(S)$	$1.76 \pm 0.36 \pm 0.18$	$-179.8 \pm 21.3 \pm 12.3$	$16.3 \pm 3.4 \pm 2.1$
$\phi(1020)$	$0.69 \pm 0.01 \pm 0.02$	$-20.7 \pm 13.6 \pm 9.3$	$19.3 \pm 0.6 \pm 0.4$
$f_0(980)$	$0.51 \pm 0.07 \pm 0.04$	$-177.5 \pm 13.7 \pm 8.6$	$6.7 \pm 1.4 \pm 1.2$
$\left[a_0(980)^0\right]$	$[0.48 \pm 0.08 \pm 0.04]$	$[-154.0 \pm 14.1 \pm 8.6]$	$[6.0 \pm 1.8 \pm 1.2]$
$f_2'(1525)$	$1.11 \pm 0.38 \pm 0.28$	$-18.7 \pm 19.3 \pm 13.6$	$0.08 \pm 0.04 \pm 0.05$
$K^*(892)^-$	$0.601 \pm 0.011 \pm 0.011$	$-37.0 \pm 1.9 \pm 2.2$	$16.0 \pm 0.8 \pm 0.6$
$K^*(1410)^-$	$2.63 \pm 0.51 \pm 0.47$	$-172.0 \pm 6.6 \pm 6.2$	$4.8 \pm 1.8 \pm 1.2$
$K^- \pi^0(S)$	$0.70 \pm 0.27 \pm 0.24$	$133.2 \pm 22.5 \pm 25.2$	$2.7 \pm 1.4 \pm 0.8$

the LASS amplitude for $K^- \pi^+ \to K^- \pi^+$ elastic scattering [28],

$$A_{K\pi(S)}(s) = \frac{\sqrt{s}}{p} \sin\delta(s) e^{i\delta(s)}, \qquad (7)$$

$$\delta(s) = \cot^{-1}\left(\frac{1}{pa} + \frac{bp}{2}\right) + \cot^{-1}\left(\frac{M_0^2 - s}{M_0 \Gamma_0 \cdot \frac{M_0}{\sqrt{s}} \cdot \frac{p}{p_0}}\right), (8)$$

where M_0 (Γ_0) refers to the $K_0^*(1430)$ mass (width), $a = 1.95 \pm 0.09$ GeV^{-1}c, and $b = 1.76 \pm 0.36$ GeV^{-1}c. The unitary nature of Eq. 7 provides a good description of the amplitude up to 1.45 GeV/c^2 (i.e., $K\eta'$ threshold). In Eq. 8, the first term is a non-resonant contribution defined by a scattering length a and an effective range b, and the second term represents the $K_0^*(1430)$ resonance. The phase space factor $\sqrt{s}/p$ converts the scattering amplitude to the invariant amplitude.

A second model uses the E791 results for the $K^- \pi^+$ S-wave amplitude from an energy-independent partial wave analysis in the decay $D^+ \to K^- \pi^+ \pi^+$ [30]. The third model uses a coherent sum of a uniform non-resonant term, and Breit-Wigner terms for the $\kappa(800)$ and $K_0^*(1430)$ resonances.

The D^0 decay to a $K^- K^+$ S-wave state is described by a coupled-channel Breit-Wigner amplitude for the $f_0(980)$ and $a_0(980)$ resonances, with their respective couplings to $\pi\pi$, $K\bar{K}$ and $\eta\pi$, $K\bar{K}$ final states [12],

$$A_{f_0[a_0]}(s) = \frac{M_{D^0}^2}{M_0^2 - s - i(g_1^2 \rho_{\pi\pi[\eta\pi]} + g_2^2 \rho_{K\bar{K}})}. \quad (9)$$

Several models are used incorporating various combinations of intermediate states. In each fit, the $K^*(892)^+$ is included and the complex amplitude coefficients of other states relative to it is measured.

The LASS $K\pi$ S-wave amplitude gives the best agreement with data and it is uses it in the nominal fits. The $K\pi$ S-wave modeled by the combination of $\kappa(800)$ (with parameters taken from Ref. [29]), a non-resonant term and $K_0^*(1430)$ has a smaller fit probability (χ^2 probability $< 5\%$). The best fit with this model (χ^2 probability 13%) yields a charged κ of mass (870 ± 30) MeV/c^2, and width (150 ± 20) MeV/c^2, significantly different from those reported in Ref. [29] for the neutral state. This does not support the hypothesis that production of a charged, scalar κ is being observed. The E791 amplitude [30] describes the
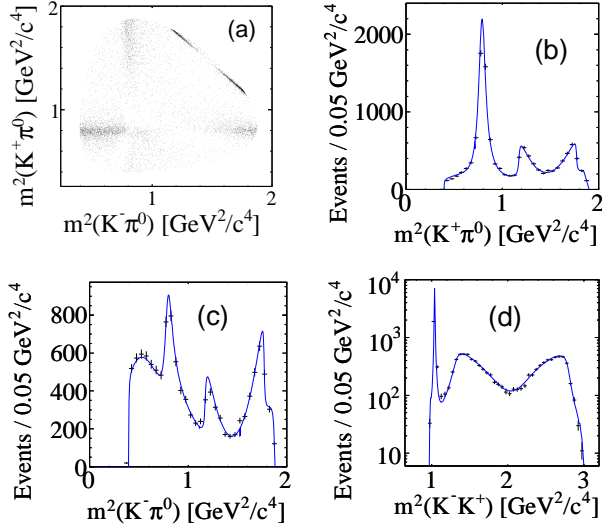
Figure 5: (Color online) Dalitz plot for $D^0 \to K^- K^+ \pi^0$ data (a), and the corresponding squared invariant mass projections (b–d). The three-body invariant mass of the D^0 candidate is constrained to the nominal value. In plots (b–d), the dots (with error bars, black) are data points and the solid lines (blue) correspond to the best isobar fit models.

data well, except near threshold (χ^2 probability 23%). Analysis of moments of $\cos\theta_H$ confirms little variation in S-wave phase up to about 1.02-1.03 GeV/c^2 and matched the behaviour obtained with the isobar model.

The results of the best fit are summarized in Table IV. Neglecting CP violation, the strong phase difference, δ_D, between the $\overline{D}^0$ and D^0 decays to $K^*(892)^+ K^-$ state and their amplitude ratio, r_D, are given by

$$r_D e^{i\delta_D} = \frac{a_{D^0 \to K^{*-}K^+}}{a_{D^0 \to K^{*+}K^-}} e^{i(\delta_{K^{*-}K^+} - \delta_{K^{*+}K^-})}. \quad (10)$$

Combining the results of models I and II, we find $\delta_D = -35.5° \pm 1.9°$ (stat) $\pm 2.2°$ (syst) and $r_D = 0.599 \pm 0.013$ (stat) ± 0.011 (syst). These results are consistent with the previous measurements [31], $\delta_D = -28° \pm 8°$ (stat) $\pm 11°$ (syst) and $r_D = 0.52 \pm 0.05$ (stat) ± 0.04 (syst).

The measurement of r_D and δ_D is a prerequisite to extract the CKM angle γ from the analysis of $B^\mp \to \tilde{D}^0 K^\pm$ decays [32], where the symbol $\tilde{D}^0$ indicates either a D^0 or a $\overline{D}^0$ meson decaying into a CP-eigenstate as $K^- K^+ \pi^0$ or $K_S^0 \pi^- \pi^+$ as we will see in more detail in the next Section.

5. Dalitz model and CKM γ extraction

Assuming no CP asymmetry in D decays the $B^\mp \to \tilde{D}^0 K^\pm$, $\tilde{D}^0 \to K_S^0 \pi^- \pi^+$, decay chain rate $\Gamma_\mp(m_-^2, m_+^2)$ can be written as

$$\Gamma_\mp(m_-^2, m_+^2) \propto |\mathcal{A}_{D\mp}|^2 + r_B^2 |\mathcal{A}_{D\pm}|^2 + \quad (11)$$
$$2\left\{ x_\mp \operatorname{Re}[\mathcal{A}_{D\mp}\mathcal{A}_{D\pm}^*] + y_\mp \operatorname{Im}[\mathcal{A}_{D\mp}\mathcal{A}_{D\pm}^*] \right\},$$

where m_-^2 and m_+^2 are the squared invariant masses of the $K_S^0 \pi^-$ and $K_S^0 \pi^+$ combinations respectively from the $\tilde{D}^0$ decay, and $\mathcal{A}_{D\mp} \equiv \mathcal{A}_D(m_\mp^2, m_\pm^2)$, with $\mathcal{A}_{D-}$ ($\mathcal{A}_{D+}$) the amplitude of the $D^0 \to K_S^0 \pi^- \pi^+$ ($\overline{D}^0 \to K_S^0 \pi^+ \pi^-$) decay. In Eq. (11) the following definitions are used, $x_\mp = r_B \cos(\delta_B \mp \gamma)$ and $y_\mp = r_B \sin(\delta_B \mp \gamma)$. Here, r_B is the magnitude of the ratio of the amplitudes $\mathcal{A}(B^- \to \overline{D}^0 K^{*-})$ and $\mathcal{A}(B^- \to D^0 K^{*-})$ and δ_B is their relative strong phase.

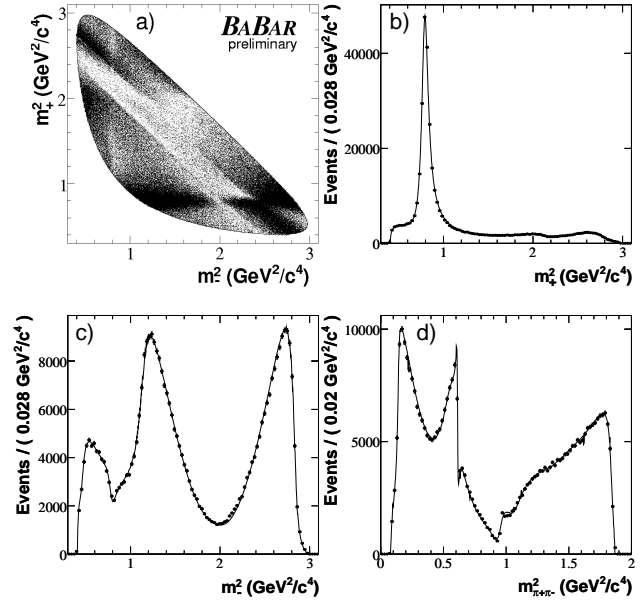Figure 6: (a) The $\overline{D}^0 \to K_S^0 \pi^- \pi^+$ Dalitz distribution from $D^{*-} \to \overline{D}^0 \pi^-$ events, and projections on (b) $m_+^2 = m_{K_S^0\pi^+}^2$, (c) $m_-^2 = m_{K_S^0\pi^-}^2$, and (d) $m_{\pi^+\pi^-}^2$. $D^0 \to K_S^0 \pi^+ \pi^-$ from $D^{*+} \to D^0 \pi^+$ events are also included. The curves are the reference model fit projections.

Once the decay amplitude $\mathcal{A}_D$ is known, the Dalitz plot distributions for $\tilde{D}^0$ from B^- and B^+ decays can be simultaneously fitted to $\Gamma_-(m_-^2, m_+^2)$ and $\Gamma_+(m_-^2, m_+^2)$ as given by Eq. (11), respectively, and the angle γ can be extracted.

Since the measurement of γ arises from the interference term in Eq. (11), the uncertainty in the knowledge of the complex form of $\mathcal{A}_D$ can lead to a systematic uncertainty.

Table V Complex amplitudes $a_r e^{i\phi_r}$ and fit fractions of the different components ($K_S^0\pi^-$ and $K_S^0\pi^+$ resonances, and $\pi^+\pi^-$ poles) obtained from the fit of the $D^0 \to K_S^0\pi^-\pi^+$ Dalitz distribution from $D^{*+} \to D^0\pi^+$ events. Errors are statistical only. Masses and widths of all resonances are taken from [22], while the pole masses and scattering data are from [34]. The fit fraction is defined for the resonance terms ($\pi\pi$ S-wave term) as the integral of $a_r^2|\mathcal{A}_r(m_-^2, m_+^2)|^2$ over the Dalitz plane divided by the integral of $|\mathcal{A}_D(m_-^2, m_+^2)|^2$. The sum of fit fractions is 1.16.

Component	$Re\{a_r e^{i\phi_r}\}$	$Im\{a_r e^{i\phi_r}\}$	Fit fraction (%)
$K^*(892)^-$	-1.159 ± 0.022	1.361 ± 0.020	58.9
$K_0^*(1430)^-$	2.482 ± 0.075	-0.653 ± 0.073	9.1
$K_2^*(1430)^-$	0.852 ± 0.042	-0.729 ± 0.051	3.1
$K^*(1410)^-$	-0.402 ± 0.076	0.050 ± 0.072	0.2
$K^*(1680)^-$	-1.00 ± 0.29	1.69 ± 0.28	1.4
$K^*(892)^+$	0.133 ± 0.008	-0.132 ± 0.007	0.7
$K_0^*(1430)^+$	0.375 ± 0.060	-0.143 ± 0.066	0.2
$K_2^*(1430)^+$	0.088 ± 0.037	-0.057 ± 0.038	0.0
$\rho(770)$	1 (fixed)	0 (fixed)	22.3
$\omega(782)$	-0.0182 ± 0.0019	0.0367 ± 0.0014	0.6
$f_2(1270)$	0.787 ± 0.039	-0.397 ± 0.049	2.7
$\rho(1450)$	0.405 ± 0.079	-0.458 ± 0.116	0.3
β_1	-3.78 ± 0.13	1.23 ± 0.16	–
β_2	9.55 ± 0.20	3.43 ± 0.40	–
β_4	12.97 ± 0.67	1.27 ± 0.66	–
$f_{11}^{\rm prod}$	-10.22 ± 0.32	-6.35 ± 0.39	–
sum of $\pi^+\pi^-$ S-wave			16.2

Two different models describing the $D^0 \to K_S^0\pi^-\pi^+$ decay have been used in this analysis. The first model (also referred to as Breit-Wigner model) [33] expresses $\mathcal{A}_D$ as a sum of two-body decay-matrix elements and a non-resonant contribution. In the second model (hereafter referred to as the $\pi\pi$ S-wave K-matrix model) the treatment of the $\pi\pi$ S-wave states in $D^0 \to K_S^0\pi^-\pi^+$ uses a K-matrix formalism [16, 17] to account for the non-trivial dynamics due to the presence of broad and overlapping resonances. The two models have been obtained using a high statistics flavor tagged D^0 sample ($D^{*+} \to D^0\pi_s^+$) selected from $e^+e^- \to c\bar{c}$ events recorded by BaBar.

In the Breit-Wigner model a set of several two-body amplitudes is used, including five Cabibbo-allowed amplitudes: $K^*(892)^+\pi^-$, $K^*(1410)^+\pi^-$, $K_0^*(1430)^+\pi^-$, $K_2^*(1430)^+\pi^-$ and $K^*(1680)^+\pi^-$, their doubly Cabibbo-suppressed partners, and eight channels with a K_S^0 and a $\pi\pi$ resonance: $\rho, \omega, f_0(980)$, $f_2(1270), f_0(1370), \rho(1450), \sigma_1$ and σ_2 . The Breit–Wigner masses and widths of the scalars σ_1 and σ_2 are left unconstrained, while the parameters of the other resonances are taken to be the same as in [33]. The parameters of the σ resonances obtained in the fit are as follows: $M_{\sigma_1} = 519 \pm 6$ MeV/c^2, $\Gamma_{\sigma_1} = 454 \pm 12$ MeV/c^2, $M_{\sigma_2} = 1050 \pm 8$ MeV/c^2 and $\Gamma_{\sigma_2} = 101 \pm 7$ MeV/c^2 (the errors are statistical only). The alternative model is based on a fit to scattering data (K-

matrix [34]) used to parametrize the $\pi\pi$ S-wave component. This variation is used to estimate the model systematic uncertainty on γ since it gives an equally good fit to data.

The error due to the resonance model can be avoided by using the model-independent γ measurement proposed in [6]. In this approach, the Dalitz plot is partitioned in bins symmetric with respect to the $\pi^+\pi^-$ axis. Counting the number of events in such bins from entangled D decay samples, in addition to the already utilized flavour-tagged D decay samples, can determine the strong phase variation over the Dalitz plot. For this the data of a τ-charm factory is needed. Useful samples consist of $\psi(3770) \to D^0\overline{D}^0$ events where one of the D mesons decays into a CP eigenstate (such as K^+K^- or $K_S^0\omega$), while the D meson going in the opposite direction decays into $K_S^0\pi^+\pi^-$. Using also a similar sample where both mesons from the $\psi(3770)$ decay into the $K^0\pi^+\pi^-$ state provides enough information to measure all the needed hadronic parameters in D decay up to one overall discrete ambiguity (this can be resolved using a Breit-Wigner model). CLEO-c showed that with the current integrated luminosity of 280 pb^{-1} at the $\psi(3770)$ resonance, these samples are already available.

With the luminosity of 750 pb^{-1}, that CLEO-c should get at the end of its operation, the samples

will be respectively about 1000 and 2000 events. Using these two samples with a binned analysis and assuming $r_B = 0.1$, a 4° precision on ϕ_3 could be obtained [35, 36].

6. Conclusions.

Charm meson multi-body decays are crucial to determine light strong interaction bound states. The nature of such mesons is still unclear, but more information is emerging from high statistics Dalitz analysis of D decays. In the future multi-channels analyses may be the way to go to identify underline structure of the light mesons. For instance a measurement of the couplings of the S-wave in various D_s decays can help in interpreting the $f_0(980)$ as two di-quark bound states [37]. Determining the decay dynamic of charm mesons is relevant for method to extract the CKM angle γ in B decays as $B^+ \to D^0 K^+$. The effect of the knowledge of the strong phase variation in charm meson decay translates into a model systematic error on the γ value. Model dependence can be removed if special sample of D meson charm decays in quantum-coherent states will be available, bringing down the model error on γ to few degrees.

Acknowledgments

References

[1] R.H. Dalitz, Philos. Mag. **44**, 1068 (1953).

[2] J.L. Rosner, Phys. Rev. **D74**, 076006 (2006); M.R. Pennington, Int. J. Mod. Phys. **D21**, 5503 (2006); D. V. Bugg, Phys. Lett. **B632**, 471 (2006).

[3] E.M. Aitala *et al.*(E791 Collaboration), Phys. Rev. Lett. **89**, 121201 (2002); E.M. Aitala *et. al* (E791 Collaboration), Phys. Rev. Lett. **86**, 770 (2001).

[4] F. E. Close and N. A. Tornqvist, J. Phys. **G28**, R249 (2002).

[5] Charge conjugation is always implied throughout the paper.

[6] A. Giri, Y. Grossman, A. Soffer, and J. Zupan, Phys. Rev. **D68**, 054018 (2003).

[7] B.Aubert et al. (BaBar Collaboration), hep-ex/0507101.

[8] S.J. Lindenbaum and R.M. Sternheimer, Phys. Rev. **105**, 1874 (1957); M.G. Olsson and G.V. Yodh, Phys. Rev. **145**, 1309 (1966); D.J. Herndon, P. Söding, and R.J. Cashmore, Phys. Rev. **D11**, 3165 (1975).

[9] W. -M. Yao *et al.* (PDG), J. Phys. **G33**, 1 (2006).

[10] J.M. Blatt and W.F. Weisskopf, Theoretical Nuclear Physics, John Wiley & Sons, New York, 1952.

[11] H. Albrecht *et al.* (ARGUS), Phys. Lett. **B308**, 435 (1993).

[12] S.M. Flatté, Phys. Lett. **B38**, 232 (1972); S.M. Flatté, CERN/EP/PHYS 76-8, 15 April 1976; S.M. Flatté Phys. Lett. B.**63**, 224 (1976).

[13] J.A. Oller, Phys. Rev. D **71**, 054030 (2005).

[14] J. Schechter, Int.J.Mod.Phys. **A20**, 6149 (2005).

[15] N.N. Achasov and G.N. Shestakov, Phys. Rev. **D 67**, 114018 (2003); N.N. Achasov and G.N. Shestakov, Yad. Fiz. **32**, 1098 (1980) [Sov. J. Nucl. Phys. **32**, 566 (1980)]; N.N. Achasov and A.A. Kozhevnikov, Phys. Rev. D **55**, 2663 (1997); N.N. Achasov and V.V. Gubin, Phys. Rev. D **56**, 4084 (1997); Yad. Fiz. **61**, 274 (1998) [Phys. Atom. Nucl. D **61**, 224 (1998)]; N.N. Achasov and A.V. Kiselev, Phys. Rev. D **70**, 111901(R) (2004); N.N. Achasov and G.N. Shestakov, Phys. Rev. D **67**, 114018 (2003); N.N. Achasov and A.V. Kiselev, Phys. Rev. D **73**, 054029 (2006).

[16] E. P. Wigner, Phys. Rev. 70 (1946) 15; S. U. Chung *et al.*, Ann. Physik 4 (1995) 404.

[17] I. J. R. Aitchison, Nucl. Phys. **A189**, 417 (1972).

[18] J.M. Link *et al.* (FOCUS Collaboration), Phys. Lett. B **585**, 200 (2004).

[19] G.Bonvicini et al. (CLEO Collaboration), Phys. Rev. D 76, 012001 (2007).

[20] P.L. Frabetti *et al.* (E687 Collaboration), Phys. Lett. B **407**, 79 (1997).

[21] J.C. Anjos *et al.* (E691 Collaboration), Phys. Rev. Lett. **62**, 125 (1989).

[22] L. Alvarez-Gaumé *et al.*, Phys. Lett. B**592**, 1 (2004).

[23] M. Ablikim *et al.* (BES Collaboration), Phys. Lett. B **607**, 243 (2005).

[24] B.Aubert et al. (BaBar Collaboration), Phys. Rev. D 72, 052008 (2005).

[25] S.U. Chung, Phys. Rev. **D56**, 7299 (1997).

[26] A. Abele *et al.*, Phys. Rev. **D57**, 3860 (1998).

[27] B.Aubert et al. (BaBar Collaboration), submitted to Phys. Rev. D.

[28] D. Aston *et al.* (LASS), Nucl. Phys. **B296**, 493 (1988); W.M. Dunwoodie, private communication.

[29] E.M. Aitala *et al.* (E791 Collaboration), Phys. Rev. Lett. **89**, 121801 (2002).

[30] E.M. Aitala *et al.* (E791 Collaboration), Phys. Rev. **D73**, 032004 (2006); B.T. Meadows, private communication.

[31] C. Cawlfield *et al.* (CLEO), Phys. Rev. **D74**,

031108 (2006).

[32] I. Dunietz, Phys. Lett. B **270**, 75 (1991); I. Dunietz, Z. Phys. **C56**, 129 (1992); D. Atwood, G. Eilam, M. Gronau and A. Soni, Phys. Lett. B **341**, 372 (1995); D. Atwood, I. Dunietz and A. Soni, Phys. Rev. Lett. **78**, 3257 (1997).

[33] CLEO Collaboration, S. Kopp *et al.*, Phys. Rev. D **63**, 092001 (2001); CLEO Collaboration, H. Muramatsu *et al.*, Phys. Rev. Lett. **89**, 251802 (2002); Erratum-ibid: **90** 059901 (2003).

[34] V. V. Anisovich and A. V. Sarantev, Eur. Phys. Jour. A **16**, 229 (2003).

[35] A. Bondar and A. Poluektov, Eur. Phys. J. C **47**, 347 (2006) [arXiv:hep-ph/0510246].

[36] A. Bondar and A. Poluektov, arXiv:hep-ph/0703267.

[37] L. Maiani, A. D. Polosa and V. Riquer, arXiv:hep-ph/0703272.

80

70

60

50

40

30

20

10

0

Format Problems, source edited

Bad or no PostScript file

Bad Fonts

Figure Problems

Unreadable disks/missing files

Paper too long

Equation problems

Author requested changes

Pages numbered/empty etc

$\overline{K}{}^{0}$

D^{0}

K^{+}

ϑ_{K}

$K^{=}$

(a)

events/20 MeV/c²

$m^2(K^{\overline{0}} K^-)$ (GeV^2/c^4)

(b)

events/6 MeV/c²

$m^2(K^+ K^-)$ (GeV^2/c^4)

(c)

events/20 MeV/c²

$m^2(K^{\overline{0}} K^+)$ (GeV^2/c^4)